

AN INTEGRAL MONITORING OF GRS1915+105: SIMULTANEOUS OBSERVATIONS WITH INTEGRAL, RXTE, THE RYLE AND NANÇAY RADIO TELESCOPES

J. Rodriguez¹, G. Pooley², D. C. Hannikainen³, and H. J. Lehto⁴

¹CEA Saclay, UMR 7158/AIM, DSM/DAPNIA/SAP, F-91191 Gif sur Yvette, France

²Cavendish Laboratory, University of Cambridge, UK

³Observatory, University of Helsinki, Finland

⁴Tuorla Observatory, Turku, Finland & Nordita, Denmark

ABSTRACT

Since the launch of *INTEGRAL* in late 2002 we have monitored the Galactic microquasar GRS 1915+105 with long exposures (~ 100 ks) pointings. All the observations have been conducted simultaneously with other instruments, in particular *RXTE* and the Ryle Telescope, and in some cases with others (Spitzer, Nançay, GMRT, Suzaku,...). We report here the results of 3 observations performed simultaneously with *INTEGRAL*, *RXTE*, the Ryle and Nançay radio telescopes. These observations show the so-called ν and λ classes of variability during which a high level of correlated X-ray and radio variability is observed. We study the connection between the accretion processes seen in the X-ray behaviour, and the ejections seen in radio. By observing ejection during class λ , we generalise the fact that the discrete ejections in GRS 1915+105 occur after sequences of X-ray hard dips/soft spikes, and identify the most likely trigger of the ejection through a spectral approach to our *INTEGRAL* data. We show that each ejection is very probably the result of the ejection of a Comptonising medium responsible for the hard X-ray emission seen above 15 keV with *INTEGRAL*. We study the rapid variability of the source, and find that the Low Frequency Quasi-Periodic Oscillations are present during the X-ray dips and show variable frequency. The ubiquity of this behaviour, and the following ejection may suggest a link between the QPO and the mechanism responsible for the ejection.

Key words: accretion, accretion disks — black hole physics — stars: individual (GRS 1915+105) — X-rays: stars — X-rays: observations (INTEGRAL, RXTE)– Radio: observations.

1. INTRODUCTION

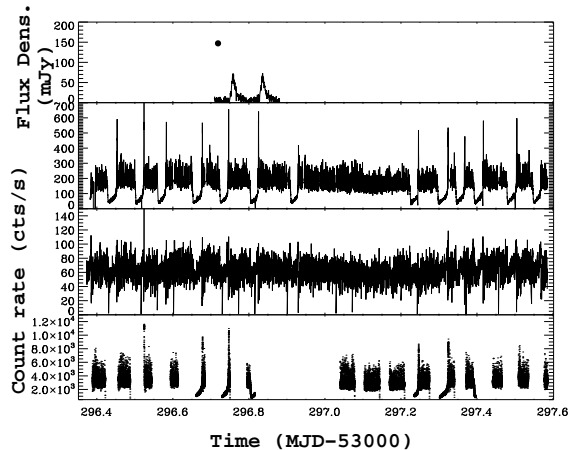
GRS 1915+105 is probably the most spectacular high energy source of our Galaxy. An extensive review on it can be found in [5]. To summarize, GRS 1915+105 is a microquasar hosting a black hole of $14.0 \pm 4.4 M_{\odot}$ [10],

it is one of the brightest X-ray sources in the sky and it is a source of superluminal ejection [13], with true velocity of the jets $\geq 0.9c$. The source is also known to show a compact jet during its periods of low steady levels of emission [e.g. 6]. Multi-wavelength coverage from radio to X-ray has shown a clear but complex association between the soft X-rays and radio/IR behaviour. Of particular relevance is the existence of radio QPO in the range 20–40 min associated with the X-ray variations on the same time scale. These so called “30-minute cycles” were interpreted as being due to small ejections of material from the system, and were found to correlate with the disc instability, as observed in the X-ray band [e.g. 14]. Extensive observations at X-ray energies with *RXTE* have allowed [2] to classify all the observations into 12 separate classes (labeled with greek names), which could be interpreted as transitions between three basic states (A-B-C): a hard state and two softer states. These spectral changes are, in most classes, interpreted as reflecting the rapid disappearance of the inner portions of an accretion disc, followed by a slower refilling of the emptied region [1].

In the X-ray timing domain, GRS 1915+105 also shows interesting features, such as the presence of Low or High Frequency Quasi-Periodic Oscillations (LFQPO, HFQPO) whose presence is, as observed in other microquasars, tightly linked the X-ray behaviour. LFQPOs with variable frequency during classes showing cycles have been reported. Correlations between the frequency and some of the spectral parameters have been pointed out [e.g. 12, 16, 17]. GRS 1915+105 is also one of the first BH systems in which the presence of HFQPOs has been observed, first at $\sim 65 - 69$ Hz, and up to ~ 170 Hz [15, 3]. Although in all cases the frequencies of all types of QPOs seem to indicate a link with the accretion disc, their presence is always associated to the presence of a hard X-ray tail in the energy spectra.

The link between the accretion and ejection processes is, however, far from being understood and different kinds of model are proposed to explain all observational facts also including the X-ray low (0.1-10 Hz) frequency QPOs. It should be added that until the launch of *INTEGRAL* all studies had been made below 20 keV with the PCA onboard *RXTE*, bringing, thus, only few

Figure 1. Multiwavelength light curves of GRS 1915+105 on October 17-18 2004 showing two interval of class ν variability. a) Ryle (line) at 15 GHz, and Nançay (point) at 2.7 GHz, b) JEM-X 3-13 keV, c) ISGRI 18-100 keV, d) RXTE 2-60 keV.



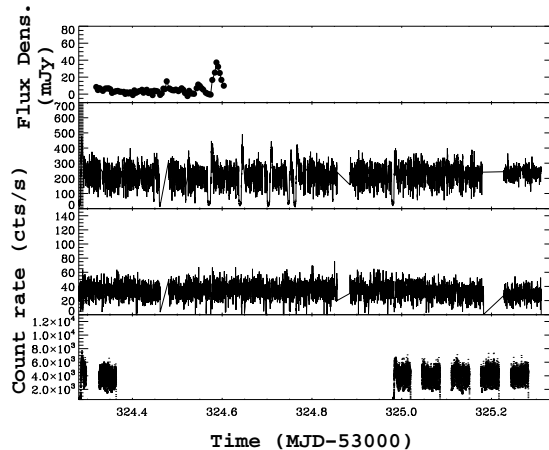
constraints to the behaviour of the hard X-ray emitter (hereafter called corona). Since the launch of *INTEGRAL* in late 2002 we have monitored the Galactic microquasar GRS 1915+105 with long exposure (~ 100 ks) pointings. All the observations have been conducted simultaneously with other instruments, in particular *RXTE* and the Ryle Telescope, and in some cases with others (Spitzer, Nançay, GMRT, Suzaku,...), with the aim to try to understand the physics of the accretion-ejection phenomena, including, for the first time, the behaviour of the source seen above 20 keV up to few hundred keV. Observations of GRS 1915+105 performed during the first year of the campaign by *INTEGRAL* and *RXTE* have been reported elsewhere [e.g. 6, 9, 19], while the *INTEGRAL* results on some of the sources in this field have been subject to several publications [8, 20, 20, 7]. We report here the results obtained during observations performed during AO2 and AO3 showing sequences of X-ray hard dips/soft spikes (the cycles), followed by radio flares. The details of these analysis and extended discussions can be found in Rodriguez et al. (2006b).

2. DESCRIPTION OF THE 3 OBSERVATIONS

We focus in this paper on 3 observations respectively taken on October 17-18 2004 (Obs. 1), November 15-16 2004 (Obs. 2), and May 13-14 2005 (Obs. 3). The multiwavelength light curves are shown in Fig. 1 to 3.

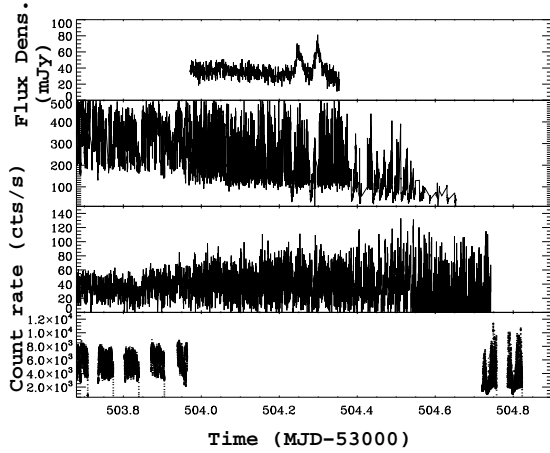
The JEM-X light curves show in all cases the occurrences of soft X-ray dips of different duration, followed by a short spike marking the return to a high degree of soft X-ray emission and variability (hereafter cycle). In all the following we focus on the moments of cycle activity and more specifically on the intervals during which we have simultaneous data at radio wavelengths, and/or

Figure 2. Multiwavelength light curves of GRS 1915+105 on November 2004 during class λ variability. The panels are the same as in Fig. 1 with the exception that no Nançay data are available.



RXTE data for the timing analysis. This is particularly relevant for Obs.1 and 3 during which transitions between different classes are seen [22]. We, therefore, avoid including in our analysis classes for which the radio behaviour is not known. These observations are classified following [2] as ν , λ , and β type cycle activity for Obs. 1, 2 and 3, respectively. In all three cases we observe at least one radio flare, which is indicative of a small ejection of material [14], after a cycle. The high flux shown by Nançay at 2.7 GHz during the class ν observation suggests that the radio flares follow systematically each cycle, as reported by [11]. The presence of radio oscillations is also known in class β , while no radio/X-ray connection had ever been observed during a class λ [11]. Despite of the similarities at soft X-ray energies (i.e. the presence of cycles) and in the radio domain (the flares), and the connection between the 2 domains, large differences remain between the 3 observations at the time of the X-ray radio connection. While in class ν the 18-100 keV light curve shows a rather high degree of hard X-ray emission, and occurrences of dips correlated with the soft X-ray dips, the level of > 18 keV emission in class λ is much lower (by a factor of ~ 2), and shows no occurrence of dips (Fig.2). In the class β observation, although the class obviously changes along the observation, the level of hard X-ray seems to remain roughly constant. The degree of variability, however, evolves and increases. Hard X-ray dips correlated to the softer ones appear. As in class ν the amplitude of the variation between the pre-dip level and the dip level is lower than that seen at softer X-rays. This behaviour had also been pointed out by [16] during a class α observation.

Figure 3. Multiwavelength light curves of GRS 1915+105 on May 2005 with the appearance of class β variability half way through the observation. The panels are the same as in Fig. 2.



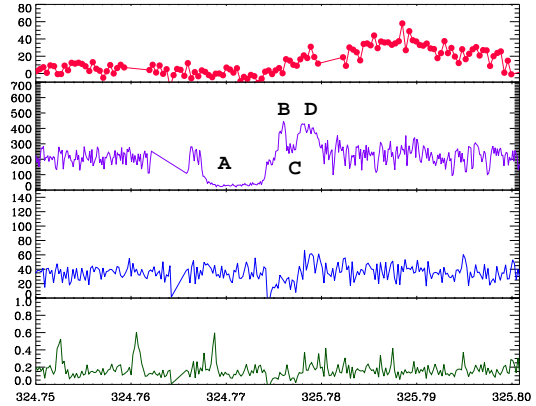
3. X-RAY SPECTRAL ANALYSIS

3.1. Selection of Good Time Intervals

In order to study the spectral evolution of GRS 1915+105 through the cycle and the possible origin of the radio ejection, we divided the cycles into different intervals from which JEM-X and ISGRI spectra were accumulated. Each cycle was divided in, at least, 3 intervals based on the soft X-ray count rate and the 3-13/18-100 keV hardness ratio. The intervals are defined as follow:

- Class ν : each cycle is composed of 4 distinct features. The soft X-ray dip, having a hard spectrum (interval ν_A), a short precursor spike (interval ν_B), a short dip (interval ν_C) and the main spike (interval ν_D), the last 3 having soft spectra. Given the observation of radio oscillations [11], i.e. the occurrence of radio flares after each cycle, the different intervals from all cycles were further accumulated together before the fitting to increase the statistics.
- Class λ : inspection of the cycle shows slight differences here, with, in particular, occurrences of a pair of cycles at some moments, while at other intervals the cycles are isolated. Since no X-ray/radio connection had been observed in this class before, we extracted spectra from the unique cycle that is followed by an ejection. As in class ν this cycle can be divided into 4 intervals, (intervals λ_A , λ_B , λ_C , λ_D respectively represent the dip, a precursor spike, a short dip, and the main recovery spike (see Fig.4).
- The spectral behaviour of class β has been extensively studied at soft X-ray energy [e.g 12, 17], detailed analysis of the *INTEGRAL* data will be presented in [22]. Here 3 intervals can be distinguished,

Figure 4. A section on the X-ray cycle followed by the radio flare from class λ . The 4 intervals from which the spectra were accumulated (see text) are indicated. From top to bottom, the panels respectively represent the Ryle light curve, the 3-13 keV JEM-X light curve, the 18-100 keV ISGRI light curve, and the 18-100/3-13 keV hardness ratio.



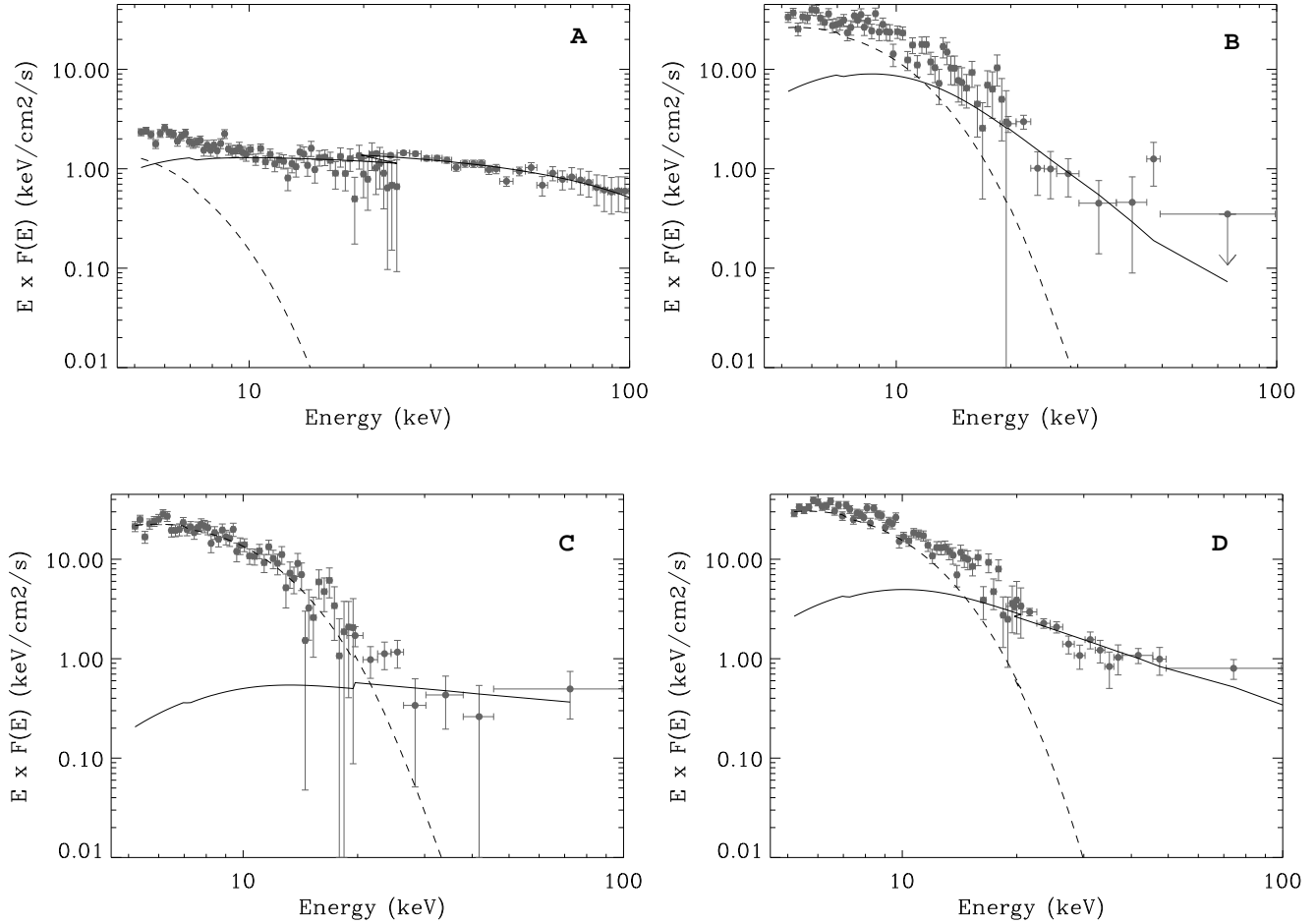
the dips, a precursor spike followed by another dip of longer duration than in the previous classes, and the major spike. As in the previous classes, the first dip is hard, while all remaining intervals have soft spectra [2].

Note the A, B, C, D labels for the different intervals are not related to the spectral states (A, B and C) identified by [2]. In order to be able to compare the different spectra, we fitted them all with the same model consisting of a thermal component (*ezdisk*) and a Comptonised one (*comptt*). Fig. 5 shows, as an example, the sequence of spectra from class λ .

3.2. Results

In all cases the evolution of the source through the cycles is more pronounced in the soft X-rays (Fig. 1 to 3). At first sight we could think that the variations are then caused by changes in the accretion disc rather than in the Comptonised component. When fitting the different spectra with physical models, however, it seems to be the contrary. In class ν evolution through ν_A to ν_D translates into an apparent approach of the accretion disc, with an increasing temperature (disc undetectable in ν_A , and reaching ~ 2.1 keV with the inner radius $R_{in} \sim 6 R_G$ (Schwarzschild radius) in ν_D). Interestingly between ν_B and ν_C , the disc seems to get closer (12 to 6 R_G), and hotter (1.21 to 1.5 keV), or at least remains constant within the errors. We calculated the 3-50 keV unabsorbed fluxes of the two spectral components in the 4 intervals. While the flux from the disk increases through the whole sequence, that of the Comptonised component is not that regular. It first increases from ν_A to ν_B before decreasing

Figure 5. The 4 spectra and best models superimposed from class λ . The individual components are also shown. The disc component is represented by the dashed line, while the Comptonised component is represented by the solid line. The evolution through the dips is quite obvious, with in particular a spectacular drop in the Comptonised component between B and C.



by a factor of 2.5 in ν_C (reaching $1.0 \times 10^{-8} \text{ erg cm}^{-2} \text{ s}^{-1}$), and slowly recovers in ν_D ($1.5 \times 10^{-8} \text{ erg cm}^{-2} \text{ s}^{-1}$).

The same behaviour is also observed in class λ . While the transition between λ_B , λ_C and λ_D is marked by a relatively constant value of the temperature of the accretion disc (around 1.8-2 keV) and the inner radius (5-7 R_G), a spectacular evolution of the Comptonised component, in particular between λ_B and λ_C is observed (this is exemplified by Fig. 5). The evolution of the 3-50 keV unabsorbed fluxes, follows the same pattern as in class ν . During the dip the 3-50 keV disc flux represents $\sim 30\%$ of the 3-50 keV flux, its contribution increases greatly during the other intervals (it is always greater than 70% of the 3-50 keV flux). Between λ_B and λ_C , the 3-50 keV flux of the Comptonised component is reduced by a factor of ~ 11 (from $2.2 \times 10^{-8} \text{ erg cm}^{-2} \text{ s}^{-1}$ to $0.19 \times 10^{-8} \text{ erg cm}^{-2} \text{ s}^{-1}$), when we leave all spectral parameters free to vary, and with a lower limit of 2.7 (if the disc temperature is frozen to the same value as in λ_B). Again after λ_C the

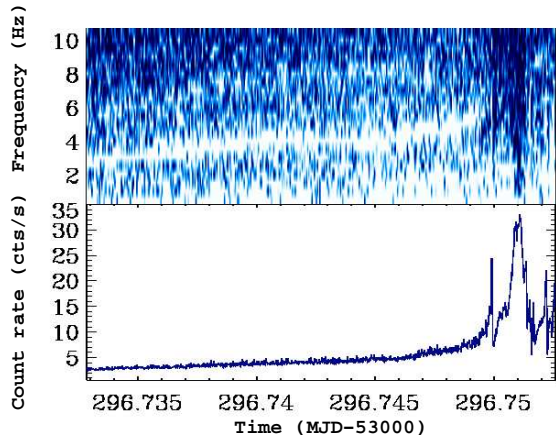
Comptonised component slightly recovers ($1.32 \times 10^{-8} \text{ erg cm}^{-2} \text{ s}^{-1}$).

The spectral behaviour of the source during class β has been extensively studied in the past. It is interesting to note that, as for the previous two classes, the disc temperature slowly increases during the dip, even after the spike [e.g. 23], while the inner radius remains small, indicating the disc is close to the compact object. The transition, after the spike, to state A [2] the very soft spectral state of GRS 1915+105, suggests that the spectacular changes occurring at the spike are related to the Comptonised component.

4. TIMING ANALYSIS: LOW FREQUENCY QPOS

Although most of the cycles seen with *RXTE* were not simultaneous with the cycles followed by radio ejections,

Figure 6. Dynamical power spectrum (top) and *RXTE*/PCA light curve (bottom) on a portion of a cycle from class ν . This cycle is one of the two for which a radio ejection is observed.



we produced dynamical power spectra of the cycles with the view to study whether or not the soft X-ray dips were associated with LFQPO of variable frequency, as been seen in class β , and α , ν and θ [e.g. 16, 17, 26]. Fig. 6 shows the dynamical power spectrum of class ν together with the associated light curve of the unique *RXTE* cycle simultaneous with the presence of radio ejection. The presence of a LFQPO (the thick white line) of varying frequency is quite obvious during the X-ray dip. The LFQPO remain until the precursor spike, and then disappears. As observed in other classes [16, 17, 26], the frequency slowly increases during the dip, following the slow increase of the source count rate.

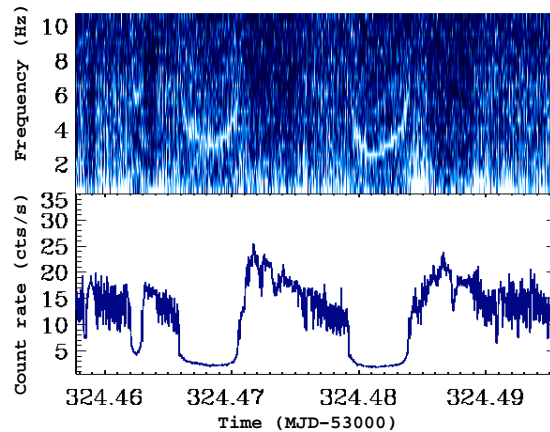
The dip preceding the radio ejection during class λ was unfortunately not covered by *RXTE*. Assuming the same pattern repeats during all dips, we extracted a dynamical power spectrum from the unique sequence of dip covered by *RXTE*. This is shown in Fig. 7 together with the associated light curve.

As in the other classes showing soft X-ray dips, a strong QPO with variable frequency appears during the dip (Fig. 7). Here, however, the frequency seems less tightly correlated to the X-ray count rate, since while during the dips the count rate remains rather constant, the frequency of the QPO is less stable.

5. DISCUSSION AND CONCLUSION

We have presented observations of GRS 1915+105 made in simultaneity with *INTEGRAL*, *RXTE*, the Ryle telescope and on one occasion the Nançay telescope. These observations belong to classes ν , λ , and β , which have the characteristic of showing sequences of soft X-ray dips followed by high level of X-ray emission with high variability, sequences we referred to as cycles. While in some

Figure 7. Dynamical power spectrum (top) and *RXTE*/PCA light curve (bottom) on the unique 2 cycles from class λ covered by *RXTE*.



of these classes ejections (observed in the radio domain) had been observed to follow to recovery to a high level of X-ray emission [e.g. 14], the observation of a radio flare during the class λ observation is, to our knowledge, the first ever reported. This allows us to generalise the fact that there is always an ejection following a cycle, provided the X-ray dip is long enough [11]. The duration of the dip during class λ is 500s, while it is as low as 330s during class β . This duration is in agreement with the results of [11] who observed that for an ejection to occur a > 100 s hard state must occur.

Detailed inspection of the cycles shows that the sequences are not as simple as it seems at first sight, but that in all cases a precursor spike occurs prior to the recovery to the high X-ray level. Our spectral analysis of the different portions of the cycles shows that the same evolution roughly occurs during the cycles from different classes. During the X-ray dip the source is in its hard state (or so-called C state for GRS 1915+105 [2]). The precursor spikes correspond to a simultaneous softening of the source spectrum and an increase in the flux of the two main spectral components, the disc and the corona. The short dip immediately following the precursor corresponds to the disappearance of the corona in the two cases we analysed in detail. The same had been observed in the case of class β [4]. Given the observation of ejected material soon after, we conclude that:

- 1) **The ejected material is the coronal material**
- 2) **The true moment of the ejection is the precursor spike**

It has to be noted that [4, 17, 26] had come to similar conclusions during other classes. Another point compatible with this scenario is that if we estimate the lag between the radio and the X-ray, we obtain 0.28h and 0.26h during class ν , 0.31h in class λ , and 0.29 and 0.34h during class β , therefore the delay is comparable in all classes. Interestingly the same conclusion had been drawn in another microquasar XTE J1550–564. During its 2000 outburst [18] have shown that the discrete ejection following the

maximum of the X-ray emission was compatible with the ejection of the coronal medium.

Although the physical properties of the dips are not exactly the same, some other similarities raise interesting questions. The timing analysis of the classes showing cycles all show the presence of a transient LFQPO appearing during the dip, and with a variable frequency which may be somehow correlated to the X-ray flux [23, 16, 17, 26]. The presence of LFQPO during hard states is quite common, and may be a signature of the physics occurring during the accretion and the ejection of matter, since a steady compact jet is usually associated with this state. In the case of the cycles, the situation may be quite different. The hard state is short and no compact jet is observed. Instead, a discrete ejection seems to take place at the end of each cycle. The presence of LFQPO during the dip may, again, indicate that the QPO phenomenon and the accretion-ejection physics are linked. Recently [25] have proposed a “magnetic flood” scenario in trying to explain the occurrence of dips and ejections, based on a magnetic instability, the Accretion Ejection Instability [24, AEI,]. This instability has the effect of transporting angular momentum and energy from the inner region of the disc, and emitting them perpendicularly and directly into the corona. A strong observational signature of this AEI is the presence of LFQPOs. In this framework the X-ray dip would correspond to the appearance of the AEI (equivalent to a transition to a hard state with appearance of LFQPO), and the ejection could be due to a reconnection event in the inner region of the disc [25]. An effect of the latter would be to blow the corona and would end observationally as an ejection. Although none of our results brings proof of such a scenario, and that other models exist, this scenario is compatible with our results. In particular with the generalisation of the ejection during all classes with dips, the relative similarities between the dips of all classes, both at radio and X-ray energies, and the constant presence of LFQPO during the dips, we feel that this model is a very promising one.

ACKNOWLEDGEMENTS

These results are presented on behalf of a much larger collaboration whose members the authors deeply thank. JR is extremely grateful to J. Chenevez, and C.-A. Oxborrow for their precious help with the JEM-X data reduction, and M. Tagger for a careful reading of an early version of this paper. JR acknowledges E. Kuulkers and E. Smith and more generally the *INTEGRAL* and *RXTE* planning teams for their great efforts to have both satellites observing GRS 1915+105 and IGR J19140+0951 at the same time.

REFERENCES

[1] Belloni, T., Mendez, M., King, A. R., et al. 1997, *ApJ*, 488, 109

- [2] Belloni, T., Klein-Wolt, M., Mendez, et al. 2000, *A&A*, 355, 271
- [3] Belloni, T., Soleri, P., Casella, P., Méndez, M., Migliari, S. 2006, *MNRAS* 369, 305.
- [4] Chaty, S. 1998, Thèse de Doctorat “Etude multi-longueur d’onde du microquasar GRS 1915+105 et de sources binaires de haute énergie de la Galaxie”
- [5] Fender, R.P. & Belloni, T. 2004, *ARA&A*, 42, 317
- [6] Fuchs, Y., Rodriguez, J., Mirabel, F., et al. 2003, *A&A*, 409, L35.
- [7] Fritz, S., Kreykenbohm, I., Wilms, J., et al. 2006, accepted in *A&A*, astro-ph 0608518.
- [8] Hannikainen, D., Rodriguez, J., Cabanac, C. et al. 2004, *A&A*, 423, p. L17
- [9] Hannikainen, D., Rodriguez, J., Vilhu, O. et al. 2005, *A&A*, 435, 995
- [10] Harlaftis, E.T & Greiner, J., 2004, *A&A*, 414, 13.
- [11] Klein-Wolt, M., Fender, R. P.; Pooley, G. G., et al. 2002, *MNRAS*, 331, 745
- [12] Markwardt, C.B., Swank, J. H., Taam, R. E. 1999, *ApJ*, 513, 37.
- [13] Mirabel, I.F. & Rodríguez, L.F. 1994, *Nature*, 371, 46
- [14] Mirabel, I.F., Dhawan, V., Chaty, S., et al. 1998, *A&A*, 330, L9
- [15] Morgan, E.H., Remillard, R.A & Greiner, J. 1997, *ApJ*, 482, 993
- [16] Rodriguez, J., Durouchoux, P., Tagger, M., et al., 2002a, *A&A*, 386, 271
- [17] Rodriguez, J., Varnière, P., Tagger, M., Durouchoux, P. 2002b, *A&A*, 387, 487
- [18] Rodriguez, J., Corbel, S., & Tomsick, J.A., 2003, *ApJ*, 595, 1032
- [19] Rodriguez, J., Corbel, S., Hannikainen, D.C., et al. 2004, *ApJ*, 615, 416
- [20] Rodriguez, J., Cabanac, C., Hannikainen, D.C., et al. 2005, *A&A*, 432, 235
- [21] Rodriguez, J., Shaw, S.E. & Corbel, S. 2006a, *A&A*, 451, 1045
- [22] Rodriguez, J., et al. 2007, submitted to *ApJ*
- [23] Swank, J.H., Chen, X., Markwardt, C., Taam, E. 1998 proceedings of the conference “Accretion Processes in Astrophysics: Some Like it Hot”, eds. S. Holt and T. Kallman
- [24] Tagger, M. & Pellat, R. 1999, *A&A*, 349, 1003
- [25] Tagger, M., Varnière, P., Rodriguez, J. & Pellat, R. 2004, *ApJ*, 607, 410
- [26] Vadawale, S.V., Rao, A.R., Naik, S., Yadav, J.S., Ishwara-Chandra, C.H., Pramesh Rao, A. and Pooley, G.G. 2003, *ApJ*, 597, 1023